Second quantization and atomic spontaneous emission inside one-dimensional photonic crystals via a quasinormal-modes approach

S. Severini,[1,2] A. Settimi,[1] C. Sibilia,[1] M. Bertolotti,[1] A. Napoli,[2] and A. Messina[2]
[1]*INFM at Dipartimento di Energetica, Università "La Sapienza" di Roma, Via Scarpa 16, 00161, Roma, Italy*
[2]*INFM and Dipartimento di Scienze Fisiche ed Astronomiche, Università di Palermo, Via Archirafi 36, 90123 Palermo, Italy*
(Received 10 March 2004; published 23 November 2004)

An extension of the second quantization scheme based on the quasinormal-modes theory to one-dimensional photonic band gap (PBG) structures is discussed. Such structures, treated as double open optical cavities, are studied as part of a compound closed system including the electromagnetic radiative external bath. The electromagnetic field inside the photonic crystal is successfully represented by a new class of modes called quasinormal modes. Starting from this representation we introduce the Feynman's propagator to calculate the decay rate of a dipole inside a PBG structure, related to the density of modes, in the presence of the vacuum fluctuations outside the one-dimensional cavity.

DOI: 10.1103/PhysRevE.70.056614 PACS number(s): 42.70.Qs, 42.50.Ct, 42.50.Nn, 11.10.Nx

I. INTRODUCTION

Photonic crystals can be viewed as particular optical cavities having the properties of presenting allowed and forbidden bands for the electromagnetic radiation traveling inside, at optical frequencies. For these motivations these structure are also named photonic band gap (PBG) [1]. In these structures, dispersive properties are usually evaluated assuming infinite periodic conditions [2]. The finite dimensions of PBGs conceptually modify the calculation and the nature of the dispersive properties: this is mainly due to the existence of an energy flow into and out of the crystal. A phenomenological approach to the dispersive properties of 1D PBG has been presented in Ref. [3]. The application of the effective-medium approach is discussed, and the analogy with a simple Fabry-Pérot structure is developed by Sipe *et al.* in Ref. [4].

The theory of quasinormal modes (QNM) [5] was been introduced by Leung *et al.*, in order to describe the electromagnetic field in one side open optical cavities. In these open systems, in fact, because of the leakage, the "modes" of the cavity are characterized by complex eigenfrequencies and for this reason they are referred to as quasinormal modes [5]. Recently this classical theory it has been extended to optical cavities open from both sides and in particular to 1D PBG cavities [6]. The purpose of this paper consists in the extension of the second quantization scheme QNM based, first introduced by Leung [7,8], to photonic band gap structures considered as double open optical cavities and this is a natural continuation of the classical work [6]. We find expressions of field correlator functions, as a formal application of the just introduced formalism, in order to investigate the problem of spontaneous emission of an atom inside the 1D-PBG structure.

In the free space, quantization of a closed cavity can be performed by using normal modes [9] where a plane wave-based operator expansion of the field is used. An open cavity, viewed as a dissipative system, cannot be quantized unless [10] one consider the bath being part of the total universe. Different methods of description of these systems are discussed in [11,12], but the starting points of this work are very different. Some of these differences (between pseudomodes [11] and the quasinormal modes) will be discussed later in this work. It has already been made an essential first step towards the application of QNMs to cavity quantum electrodynamics phenomena [7]. The second quantization of a scalar field in an open cavity is formulated, from first principles, in terms of the QNMs, which are the eigensolutions of the evolution equation, decaying exponentially in time as energy leaks to outside [7].

The behavior of systems coupled to dissipative reservoirs represents a central theme of quantum optics. Technological developments, in the form of high quality and high cavity finesse, led to the extension of such studies also into another direction, which has come to be known as cavity QED. Spontaneous and stimulated emissions are fundamental processes resulting from the interaction between radiation and matter. They depend not only on the properties of the excited atomic system but also on the nature of the environment to which the system is optically coupled. Spontaneous emission in a one-dimensional Fabry-Pérot-type optical cavity is analyzed quantum mechanically in Ref. [13]; this link with the density of modes has been put into evidence in Ref. [14], in particular the theory of spontaneous emission from an initially excited two-level atom in a one-dimensional optical cavity with output coupling from both sides is developed in Ref. [15].

It is well known that one of the more interesting features of PBG structures is their ability to alter the spontaneous emission of probe atoms embedded in the periodic lattice; this is due to the electromagnetic field modification induced by the structure [16]. Large enhancement and complete inhibition of atomic spontaneous emission can be obtained. It was in 1946 that Purcell [17] first predicted that nontrivial boundary conditions on electromagnetic field in the vicinity of an excited atom could alter its decay rate. In the wake of theoretical promulgation of PBG structures, concern has turned to the question of the behaviour of atomic decay rate in such structures [18]. In particular, it was predicted that the decay rate could be suppressed for atoms located inside PBG

when their resonant emission frequency was in the photonic band gap. In this frequency range, the electromagnetic density of modes (DOM) is very small. Resonance enhancement of decay rate was expected at the photonic band edges where the DOM was anomalously large. In fact, the DOM and the electromagnetic modal fields are altered at the position of the atom. Reference [19] considers a more sophisticated model of atomic spontaneous emission and classical radiation in a finite 1D-PBG. The full three-dimensional (3D) or two-dimensional (2D) problem is reduced to a finite one-dimensional (1D) model, which is analytically solved by using algebraic transfer matrix techniques [20]. In Ref. [21], atomic spontaneous emission, in one-dimensional photonic band-gap structures, is numerically investigated. Both the temporal and spatial dynamics of the electromagnetic field and the atomic polarization are treated by a propagation method that allows up to easily and realistically model material boundary conditions for finite structures.

Therefore although a full analysis of the spontaneous emission process should be performed in a 3D geometry, we would like to put into evidence how the QNM approach, limited to 1D open (finite) structure, is consistent with results already known in literature [19,20], thank to the possibility of the introduction of definition of density of modes.

The present paper is organised as follows. In Sec. II, the QNM approach is introduced and briefly compared with the theory of damped harmonic oscillators [22]. In Sec. III, the essential extension of the second quantization is provided for one dimensional double open cavities, by using a Lagrangian approach [23] and introducing two driving functions that take into consideration the effect of the external space to the cavity. In Sec. IV, field correlation functions and the Feynman propagator is introduced [24,25], in order to calculate the decay rate of an atom inside an open cavity, in presence of the vacuum fluctuations outside the cavity. In Secs. V and VI, an application to a quarter-wave symmetric 1D-PBG is reported and the results are discussed.

II. QUASINORMAL MODES APPROACH

The concept of quasinormal modes has been developed for open systems wherein the electromagnetic field satisfies the wave equation [8,5]:

$$\left[\frac{\partial^2}{\partial x^2} - \rho(x)\frac{\partial^2}{\partial t^2}\right]\phi(x,t) = 0, \tag{1}$$

where $\rho(x)=[n(x)/c]^2$, with $n(x)$ the refractive index of the material and c the vacuum light speed.

The evolution equation (1) is defined in a finite interval $C=[0,d]$, representing the geometry of the finite open cavity. Attention is restricted to systems having a discontinuity in $x=0$ and $x=d$ (say steps), and no tail beyond $x=0$ and $x=d$, i.e. [6],

$$\rho(x) = \rho_0 \text{ for } x < 0, x > d, \tag{2}$$

where $\rho_0=[n_0/c]^2$, and n_0 is the outside refractive index.

Quasinormal function space is defined through Eq. (1) in association with the following outgoing wave conditions

$$\partial_x\phi(x,t) = \sqrt{\rho_0}\partial_t\phi(x,t) \text{ for } x < 0,$$

$$\partial_x\phi(x,t) = -\sqrt{\rho_0}\partial_t\phi(x,t) \text{ for } x > d. \tag{3}$$

Due to the above conditions (3), the electromagnetic spectrum becomes discrete; heuristically, the eigenfrequencies are spaced by $\Delta\omega \approx \pi c/d$. Computationally and conceptually, this discreteness is much more convenient than dealing with the infinite space of the universe, for which the spectrum would be continuous in ω. The consequence is that inside the finite space of the cavity, energy is no longer conserved, and mathematically the time evolution operator is no longer hermitian.

However the general function satisfying Eqs. (1) and (3) and can be written as [6]

$$\varphi(x,t) = \sum_n a_n\varphi_n(x,t) = \sum_n a_n f_n(x)e^{-i\omega_n t}, \tag{4}$$

where a_n are suitable coefficients, $f_n(x)$ are the quasinormal mode functions, and ω_n are the correspondent frequencies with Im $\omega_n<0$. The couple $[f_n(x),\omega_n]$ has to satisfy the following equation [8,5]:

$$\left[\frac{d^2}{dx^2} + \omega_n^2\rho(x)\right]f_n(x) = 0. \tag{5}$$

In QNM's space, the norm of the quasinormal function is a complex number and it is given by the following expression [6]:

$$\langle f_n|f_n\rangle = 2\omega_n\int_0^d \rho(x)f_n^2(x)dx + i\sqrt{\rho_0}[f_n^2(0) + f_n^2(d)], \tag{6}$$

where the main differences with the ordinary definition of norm [9] is the presence of $f_n^2(x)$ rather than $|f_n(x)|^2$ and the two additive "surfaces terms" $i\sqrt{\rho_0}f_n^2(0)$ and $i\sqrt{\rho_0}f_n^2(d)$.

It is interesting to observe that for each single QNM function $\varphi_n(x,t)$, (4) i.e., [8,5],

$$\varphi_n(x,t) = f_n(x)e^{-i\omega_n t}, \tag{7}$$

three appropriate real constants m, γ and k exist in such a way that $\varphi_n(x,t)$ satisfies the following damped harmonic oscillator equation [22]

$$m\partial_{tt}\varphi_n + \gamma\partial_t\varphi_n + k\varphi_n = 0. \tag{8}$$

This point can be easily understood substituting Eq. (7) into Eq. (8), obtaining

$$m(\omega_{nR}^2 - \omega_{nI}^2) - \gamma\omega_{nI} - k = 0,$$

$$2m\omega_{nR}\omega_{nI} + \gamma\omega_{nR} = 0, \tag{9}$$

which is an always solvable system, where the complex frequency ω_n has been decomposed in its real and imaginary parts $\omega_n=\omega_{nR}+i\omega_{nI}$ (with $\omega_{nR}=\text{Re}\,\omega_n$ and $\omega_{nI}=\text{Im}\,\omega_n$). In conclusion, the temporal behavior expressed by Eq. (7) is strictly similar to the one coming from the damped harmonic oscillator theory [22]. For the QNM theory, however, the origin of damping is not the presence of a first order time derivative for the field; but the escape of energy from the

two sides of the structure, due to the outgoing wave conditions (3).

III. SECOND QUANTIZATION

Let us now consider an open cavity of length d, filled with a medium having a refractive index space dependent $n(x)$, in the presence of two e.m. input fields, one $\phi_{left}(x,t)$ coming from the left side, the other $\phi_{right}(x,t)$ from the right side.

If the refractive index satisfies conditions (2) (see [8,6]), the QNMs form a complete basis only inside the cavity, and the e.m. field can be calculated as a superposition of QNMs [7]

$$\phi(x,t) = \sum_n a_n(t) f_n^N(x) \text{ for } 0 \leqslant x \leqslant d, \tag{10}$$

where the apex N reminds that $f_n^N(x) = f_n(x)\sqrt{2\omega_n/\langle f_n | f_n\rangle}$ are the normalized QNM functions. We can see that Eq. (10) is an extension (generalization) of previous Eq. (4). In fact, the superposition coefficients $a_n(t)$ satisfy the dynamic equation [7]

$$\dot{a}_n(t) + i\omega_n a_n(t) = \frac{i}{2\omega_n\sqrt{\rho_0}}[f_n^N(0)b_{left}(t) + f_n^N(d)b_{right}(t)], \tag{11}$$

where two driving forces $b_{left}(t)$ and $b_{right}(t)$ are linked to the incoming (real) fields $\phi_{left}(x,t)$ and $\phi_{right}(x,t)$ coming respectively from the left and right side [7]. The relation between these quantities are given by

$$b_{left}(t) = -2\sqrt{\rho_0}\,\partial_x\phi_{left}(x,t)|_{x=0},$$

$$b_{right}(t) = 2\sqrt{\rho_0}\,\partial_x\phi_{right}(x,t)|_{x=d}. \tag{12}$$

Of course the boundary conditions satisfied by the two incoming fields $\phi_{left}(x,t)$ and $\phi_{right}(t)$ have to be given in the following form:

$$\partial_x\phi_{left}(x,t) = -\sqrt{\rho_0}\partial_t\phi_{left}(x,t) \text{ for } x \leqslant 0,$$

$$\partial_x\phi_{right}(x,t) = \sqrt{\rho_0}\partial_t\phi_{right}(x,t) \text{ for } x \geqslant d. \tag{13}$$

globally called incoming wave conditions, with respect to Eq. (3). In this new scenario it is easy to verify that expression (4) is linked to a particular case of Eq. (11), in which we have $b_{left}(t) = b_{right}(t) = 0$. From a simple inspection of Eq. (11) we see that all the QNM coefficients $a_n(t)$ are driven by the two driving forces $b_{left}(t)$ and $b_{right}(t)$; so, even if each QNM coefficient has the property $\mathrm{Im}(\omega_n) < 0$, incoming waves conditions (12) ensure the presence of quasistationary regime solutions, as well as described in [7]. The coupling between the QNM inside the cavity and the driving forces $b_{left}(t)$ and $b_{right}(t)$ is determined by the surface values of the functions $f_n^N(0)$ and $f_n^N(d)$.

It is immediate to show that the Lagrangian density for the evolution equation (1) is [23]

$$L = \{\rho(x)[\partial_t\phi(x,t)]^2 - [\partial_x\phi(x,t)]^2\}/2. \tag{14}$$

In fact, if we write down the equation of Lagrange

$$\frac{d}{dt}\left(\frac{\partial L}{\partial(\partial\phi)}\right) = \frac{\partial L}{\partial\phi} - \partial_x\left(\frac{\partial L}{\partial(\partial_x\phi)}\right), \tag{15}$$

using Eq. (14), we have

$$\frac{\partial L}{\partial(\partial_t\phi)} = \rho(x)\partial_t\varphi(x,t), \tag{16}$$

$$\frac{\partial L}{\partial\phi} = 0, \tag{17}$$

and

$$\partial_x\frac{\partial L}{\partial(\partial_x\phi)} = -\partial_{xx}\phi(x,t). \tag{18}$$

So it is clear that Eq. (14) expresses the evolution equation (1) and corresponds to the Lagrangian density. The conjugated function, with respect to the Lagrangian density (14), can be calculated as an immediate consequence of the definition [23]

$$\tilde{\phi}(x,t) \equiv \frac{\partial L}{\partial(\partial_t\phi)} = \rho(x)\partial_t\phi(x,t). \tag{19}$$

So, from Eq. (16), the conjugated function of $\phi(x,t)$ is the product of $\rho(x)$ and the time derivative $\partial_t\phi(x,t)$. The Hamilton density function associated to the evolution equation (1) is [23]

$$H = \rho(x)[\partial_t\phi(x,t)]^2 - L = \frac{[\partial_x\phi(x,t)]^2}{2} + \rho(x)\frac{[\partial_t\phi(x,t)]^2}{2}. \tag{20}$$

As discussed by Ho *et al.* [7], the cavity energy deduced by Eq. (20), in the conservative limit, does not depend on time t. The introduction of the conjugated function in Eq. (19) enables us to use this concept in the definition of the inner product as will be clear in what follows.

Our purpose is to develop a formalism whereby field quantization [9] can be implemented in terms of QNMs. This allows us to interpret the expansion coefficients $a_n(t)$ appearing in Eq. (10), as generalized annihilation and creation operators for the discrete QNMs.

Coefficients $a_n(t)$ are the expansion terms on the QNM base [8]:

$$a_n(t) = \frac{\langle f_n^N(x)|\phi(x,t)\rangle}{\langle f_n^N(x)|f_n^N(x)\rangle}, \tag{21}$$

where the inner product is given by the following expression [8]:

$$\langle\Phi(x,t)|\Psi(x,t)\rangle = i\int_0^d [\Phi(x,t)\tilde{\Psi}(x,t) + \tilde{\Phi}(x,t)\Psi(x,t)]dx + \Phi(0,t)\Psi(0,t) + \Phi(d,t)\Psi(d,t). \tag{22}$$

The tilded functions $\tilde{\Psi}$ and $\tilde{\Phi}$ are respectively conjugated to Ψ and Φ, in view of the Lagrangian (14).

Coefficients $a_n(t)$, functions $f_n^N(x)$ and frequencies ω_n satisfy symmetry properties [5]:

$$\omega_{-n} = -\omega_n^* \tag{23}$$

and [5]

$$a_{-n}(t) = a_n^*(t),\ f_{-n}^N(x) = [f_n^N(x)]^* . \tag{24}$$

So we can rewrite Eq. (10) in the following way:

$$\phi(x,t) = \sum_{n=0}^{\infty} [a_n(t) f_n^N(x) + a_n^*(t)(f_n^N(x))^*]. \tag{25}$$

The second quantization proceeds by first promoting $\phi(x,t)$ to field operator [9]. To this end, in analogy with the standard quantum expansion of the free field, where we find creation and annihilation operator multiplied by plane wave terms into a relation similar to Eq. (25) (in which functions f_n^N are substituted by e^{ikx}), functions $a_n(t)$ can be regarded as operators.

We adopt the following equal time canonical quantization rules for the field $\hat{\phi}(x,t)$ operator [9]

$$[\hat{\phi}(x,t), \hat{\dot{\phi}}(x',t)] = i\delta(x-x'). \tag{26}$$

This field may be regarded as operator for the entire universe, which is a conservative system. The same projection formula (21), as in the classical case, now defines $\hat{a}_n(t)$ and $\hat{a}_n^\dagger(t)$ as QNM-space operators, obeying the equation of motion (11). We can express the field operator $\hat{\phi}(x,t)$ in terms of the operators $\hat{a}_n(t)$ and $\hat{a}_n^\dagger(t)$ as

$$\hat{\phi}(x,t) = \sum_{n=0}^{\infty} [\hat{a}_n(t) f_n^N(x) + \hat{a}_n^\dagger(t)(f_n^N(x))^*]. \tag{27}$$

If we calculate the generic commutator between two QNMs, we have

$$[\hat{a}_n, \hat{a}_{n'}] = \frac{[\langle f_n^N(x), \phi(x,t)\rangle, \langle f_{n'}^N(x), \phi(x,t)\rangle]}{\langle f_n^N(x), f_n^N(x)\rangle \langle f_{n'}^N(x), f_{n'}^N(x)\rangle} \tag{28}$$

and by using relation (26) we have

$$[\hat{a}_n, \hat{a}_{n'}] = \frac{\omega_{n'} - \omega_n}{4\omega_n\omega_{n'}} \int_0^d \rho(x) f_n^N(x) f_{n'}^N(x) dx. \tag{29}$$

Quasinormal functions $f_n^N(x)$ are orthogonal with respect to the norm (22), so we can write [6]

$$i(\omega_n + \omega_{n'}) \int_0^d \rho(x) f_n^N(x) f_{n'}^N(x) dx = \sqrt{\rho_0}[f_n^N(0) f_{n'}^N(0) + f_n^N(d) f_{n'}^N(d)], \tag{30}$$

that is valid for $n' \neq n$. Using the relation (30), commutator (29) becomes

$$[\hat{a}_n, \hat{a}_{n'}] = \frac{\omega_{n'} - \omega_n}{4\omega_n\omega_{n'}} \frac{\sqrt{\rho_0}[f_n^N(0) f_{n'}^N(0) + f_n^N(d) f_{n'}^N(d)]}{i(\omega_n + \omega_{n'})} \tag{31}$$

that is valid only if $n' \neq n$. In order to understand better these canonical quantization rules, we can put in Eq. (31) $n' = -n$. For the relations (23) and (24) we have

$$[\hat{a}_n, \hat{a}_{-n}] = [\hat{a}_n, \hat{a}_n^\dagger] = \frac{\mathrm{Re}[\omega_n]}{2|\omega_n|^2} \int_0^d \rho(x) |f_n^N(x)|^2 dx \tag{32}$$

or equivalently

$$[\hat{a}_n, \hat{a}_n^\dagger] = -\frac{\sqrt{\rho_0}\,\mathrm{Re}[\omega_n]}{4|\omega_n|^2\,\mathrm{Im}[\omega_n]}[|f_n^N(0)|^2 + |f_n^N(d)|^2]. \tag{33}$$

In the paper [7] it is possible to find a simple demonstration in which relation (32), in the conservative and stationary limit, is $[\hat{a}_n, \hat{a}_n^\dagger] = 1/2\omega_n$. This expression is similar to the one concerning the well known annihilation ($\hat{c}_n$) and creation ($\hat{c}_n^\dagger$) operators, if we assume for the QN operators $\hat{a}_n = \sqrt{2\omega_n}\hat{c}_n$ and $\hat{a}_n^\dagger = \sqrt{2\omega_n}\hat{c}_n^\dagger$. This result can be intuitively understood observing that, when we consider the conservative limit, i.e., when we consider the limit of closed cavity (the field tends to the nodal conditions at the two ends of the structures), in Eq. (33) we have $\mathrm{Im}[\omega_n] \to 0$: this imaginary part goes to zero with the same velocity of $|f_n^N(0)|^2 + |f_n^N(d)|^2$, since the damping is related to escape of energy from the two ends of the structures.

We would like to remark that QNM approach is very different from the pseudomodes approach introduced by Dalton *et al.* [11]. In fact, the pseudomodes are obtained by the Fano transformation of the normal modes [12], so they use an ordinary metric and the canonical second quantization is adopted; QNM do not, they use a specific definition for the norm (metric) and so a noncanonical second quantization is adopted (see. Refs. [5,8,9]).

Modification of the commutation relations with respect to the canonical ones, gives rise to a modification of the emission properties of a dipole embedded in a 1D microcavity, as clearly described in the work of Ueda *et al.* [26]. We observe, from Eq. (32), that the commutation rules of QNM quasimodes exhibit a modification with respect to the canonical one, and therefore we have to expect an influence on the spontaneous emission process due to the cavity geometry.

In what follows we analyze the spontaneous emission process in 1D open cavity. Although a full analysis of the spontaneous emission process should be performed in a 3D geometry, we would like to put into evidence how this approach, limited to 1D open (finite) structure, is consistent with results already known in literature [19,20], thanks to the possibility of the introduction of definition of density of modes; we remember that the density of modes is proportional to the spontaneous emission rate of an embedded probe atom, by Fermi's golden rules.

IV. ATOMIC SPONTANEOUS EMISSION

Since the two classical incoming fields $\phi_{left}(x,t)$ and $\phi_{right}(x,t)$ introduced in the previous section are real functions, the corresponding field operators are Hermitian, hence the two driving forces in the quantum domain will become Hermitian operators too. Let us quantize these two driving forces, viewing the two fields in the quantum domain as two uncorrelated fields having only *vacuum fluctuations* [9].

In the Fourier transformed domain, Hermiticity does not hold; so the transformed driving forces operators $\hat{b}_{left}(\omega)$ and

$\hat{b}_{right}(\omega)$ are not hermitian in general. These two fields have a zero mean value $\langle \hat{b}(\omega)\rangle = 0$ but a nonzero root-mean-square deviation [7]:

$$\langle \hat{b}^{\dagger}(\omega)\hat{b}(\omega)\rangle = \overline{\mathcal{E}}(\omega) = \hbar\omega/2, \tag{34}$$

where $\hbar$ is the Planck constant.

The phenomenon of *spontaneous emission* of an atom can be considered as an *emission induced by the vacuum fluctuations*. In fact, even in absence of incident photons, an atom inside the open cavity sees the vacuum fluctuations related to the quantum mechanical nature of the electromagnetic field outside the cavity. Under the effect of these fluctuations, it can emit a photon and fall back into a lower energy state (the energy of the global system being conserved during this process).

In order to study the spontaneous decay rate of an atom inside the cavity, with the QNM formalism we have to find the correlation field functions in terms of quasinormal functions [9,7]. In what follows, we use the same procedure that Leung *et al.* have used in the contest of optical cavities open from one side only [7]. The results that we find in this section are valid for double open optical cavities and, in particular, in the next section, we apply the treatment to photonic band gap structures.

The formalism derived in the previous section for expanding the quantum electromagnetic field $\hat{\phi}(x,\omega)$ in terms of creation and annihilation operators $\hat{a}_n^{\dagger}(\omega)$ and $\hat{a}_n(\omega)$ can be applied to the calculation of equilibrium correlation functions, yielding discrete representations for the cavity field correlator:

$$\begin{aligned}\tilde{F}(x,x',\omega) &= \langle \hat{\phi}^{\dagger}(x,\omega)\hat{\phi}(x',\omega)\rangle \\ &= \overline{\mathcal{E}}(\omega)\sum_{n,n'} \frac{f_n^N(0)f_{n'}^N(0) + f_n^N(d)f_{n'}^N(d)}{4\rho_0\omega_n\omega_{n'}(\omega_n-\omega)(\omega_{n'}+\omega)} f_n^N(x)f_{n'}^N(x').\end{aligned} \tag{35}$$

The above formula (35) leads to a clear physical interpretation of pole structure in complex plane $\omega \in \boldsymbol{C}$: the QNM poles ω_n, with $\mathrm{Im}[\omega_n] < 0$, correspond to the cavity resonances excited by the vacuum fluctuations.

Another important correlation function is the Feynman propagator [25],

$$G^F(x,t,x',t') = -i\langle \mathrm{T}\{\hat{\phi}(x,t)\hat{\phi}(x',t')\}\rangle, \tag{36}$$

in which $\boldsymbol{T}$ denotes the time-ordered thermal propagator [24].

Let us now see how the form given in Eq. (36) can be interpreted [27]. First, if $t<t'$, the matrix element describes the amplitude of a particle being created at a time t, which propagates in space-time and is annihilated at a later time t'. Similarly, if $t>t'$, Eq. (36) describes the amplitude of a particle being created at a time t', which propagates in space-time and is annihilated at a later time t. This, in a sense, is the physical meaning of the propagator, which also shows why it should be important to calculate the amplitudes of various processes involving particle interactions. After all, between interactions, the particles just propagate in space-time.

Taking the Fourier transform of the definition (36) leads to a direct relation in terms of the cavity correlator (35), as from [27],

$$\begin{aligned}\tilde{G}^F(x,x',\omega) = -\lim_{\varepsilon\to 0}\int_{-\infty}^{\infty}\frac{d\omega'}{2\pi}\left(\frac{1}{\omega'+\omega-i\varepsilon}+\frac{1}{\omega'-\omega-i\varepsilon}\right) \\ \times\tilde{F}(x,x',\omega').\end{aligned} \tag{37}$$

Substitution of the right-hand side of Eq. (35) into Eq. (37) yields Feynman propagator as

$$\begin{aligned}\tilde{G}^F(x,x',\omega) = -i\frac{\hbar}{2}\sum_{n,n'}\frac{f_n^N(0)f_{n'}^N(0)+f_n^N(d)f_{n'}^N(d)}{4\rho_0\omega_n\omega_{n'}(\omega_n+\omega_{n'})} \\ \times\left[\theta(\omega)\frac{\omega_n}{\omega_n-\omega}+\theta(-\omega)\frac{\omega_{n'}}{\omega_{n'}+\omega}\right]f_n^N(x)f_{n'}^N(x'),\end{aligned} \tag{38}$$

where $\theta(\omega)$ is the unit step function.

In paper [7], it has been remarked that the nondiagonal representation of Feynman propagator in terms of QNMs has some nice properties, and it is in fact the unique representation if the field $\hat{\phi}(x,\omega)$ and the conjugate momentum $\hat{\tilde{\phi}}(x,\omega)$ are considered together. There are of course many ways to understand why the Feynman propagator is nondiagonal; one of the most direct is via the equation of motion (11) which shows that all the QNM coefficients $\hat{a}_n(\omega)$ are driven by the two driving forces $\hat{b}_{left}(\omega)$ and $\hat{b}_{right}(\omega)$, so that in general different coefficients will have phase coherence and hence a nonzero correlation. However, the cavity correlator (35) and the Feynman propagator (38) become diagonal, as they should, in the conservative limit when $|\mathrm{Im}[\omega_n]| \ll \mathrm{Re}[\omega_n]$. In agreement with the creation-annihilation interpretation of the operators $a_n(\omega)$ and $\hat{a}_n^{\dagger}(\omega)$, the conservative limit is such that

$$\langle \hat{a}_{n'}(\omega)\hat{a}_n^{\dagger}(\omega)\rangle \approx \frac{\pi}{\omega}\delta(\omega-\omega_n)\delta_{n,n'}. \tag{39}$$

It is now profitable to consider the very simple example of an atom inside the open cavity (at a point x) which is stimulated by the vacuum fluctuations outside the cavity (at frequency ω); in the dipole approximation and for weak atom-pump coupling, the decay rate is related to the equilibrium equal-space propagator [25]

$$\tilde{D}(x,\omega) \equiv \tilde{G}^F(x,x,\omega). \tag{40}$$

The conservative limit [7] is the only case in which a single QNM can dominate (narrow resonances $|\mathrm{Im}\,\omega_n| \ll |\mathrm{Re}\,\omega_n|$) and the vacuum fluctuations can be coupled to just one QNM ($\omega \simeq \mathrm{Re}[\omega_n]$); so, if the single-QNM condition $n' = -n$ is inserted into Eq. (38), the dipole at the point x is coupled to the nth QNM and the equal-space propagator becomes

$$\tilde{D}_n(x,\omega) = \frac{1}{4\sqrt{\rho_0}} \frac{\alpha_n}{|\omega_n|^2} |f_n^N(x)|^2 \left[\theta(\omega) \frac{\omega_n}{\omega - \omega_n} + \theta(-\omega) \frac{\omega_n^*}{\omega - \omega_n^*} \right], \tag{41}$$

where the normalization integrals α_n are defined and calculated as [Eq. (30)]

$$\alpha_n = \frac{1}{d} \int_0^d \rho(x) |f_n^N(x)|^2 dx = \frac{\sqrt{\rho_0}/d}{2|\mathrm{Im}\ \omega_n|} [|f_n^N(0)|^2 + |f_n^N(d)|^2]. \tag{42}$$

Only the sum of the two terms in Eq. (41) preserves the fundamental relation [9] $\tilde{D}^R(x,\omega) = [\tilde{D}^A(x,\omega)]^*$ for real ω, where $\tilde{D}^R(x,\omega)[\tilde{D}^A(x,\omega)]$ is the retarded (advanced) propagator obtained from $\tilde{D}(x,\omega)$ by continuation from positive (negative) frequencies. Moreover, $\tilde{D}(x,\omega)$ satisfies term by term the equally fundamental inequality $\mathrm{Im}[\tilde{D}(x,\omega)] \leqslant 0$ on the real axis [9]. A violation of this inequality could lead to a retardered atom propagator that has poles in the upper half plane of $\omega \in \boldsymbol{C}$, signifying an unphysical instability.

The decay rate in the open cavity $\delta_n(x,\omega)$, in units of the one in the universe [9], is physically related to the equal-space propagator $\tilde{D}_n(x,\omega)$, mathematically by the following definition [25]

$$\delta_n(x,\omega) = -\frac{2\omega\sqrt{\rho_0}}{\pi} \mathrm{Im}[\tilde{D}_n(x,\omega)], \tag{43}$$

for real positive frequencies $\omega > 0$.

Inserting Eq. (41) into Eq. (43), under the hypothesis $\omega \simeq \mathrm{Re}[\omega_n] \gg |\mathrm{Im}[\omega_n]|$, the decay rate $\delta_n(x,\omega)$ can be expressed as

$$\delta_n(x,\omega) \cong \frac{1}{2d} \frac{|f_n^N(x)|^2}{\alpha_n} \frac{\sigma_n(\omega)}{K_n}, \tag{44}$$

where $\sigma_n(\omega)$ is the global density of probability (DOM) for the nth QNM [13–15]

$$\sigma_n(\omega) = K_n \frac{d}{\pi} \frac{\alpha_n^2 |\mathrm{Im}\ \omega_n|}{(\omega - \mathrm{Re}\ \omega_n)^2 + \mathrm{Im}^2\ \omega_n}, \tag{45}$$

Equations (44) and (45) confirm the validity of the QNM approach; in fact, the Fermi's golden law has been obtained: if a dipole inside the open cavity (x-point) is stimulated by the vacuum fluctuations outside the cavity (ω-frequency) which are coupled just to the nth QNM, then the decay rate $\delta_n(x,\omega)$ is proportional, in particular, to the QNM intensity $|f_n^N|^2$ in the point x, and also to the DOM σ_n at the frequency ω.

Under the hypothesis of narrow resonances $|\mathrm{Im}\ \omega_n| \ll |\mathrm{Re}\ \omega_n|$ the normalization integrals can be approximated to $\alpha_n \cong 1/d$, and the normalization constants K_n can be obtained by the following condition

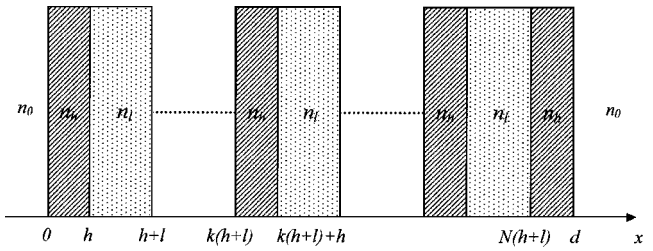

FIG. 1. Refractive index $n(x)$ for a symmetric 1D-PBG with N periods plus one layer; every period is composed by two layers, having respectively lengths h and l and refractive indices n_h and n_l. The added layer has parameters h and n_h.

$$\int_{\mathrm{Re}\ \omega_n - \Delta\omega_n}^{\mathrm{Re}\ \omega_n + \Delta\omega_n} \sigma_n(\omega) d\omega = \frac{1}{d}. \tag{46}$$

In fact, in the cavity of length d, the dipole is coupled just to the nth QNM, with resonance $\mathrm{Re}\ \omega_n \geqslant 0$ and around $2\Delta\omega_n \ll \mathrm{Re}\ \omega_n$, where $\Delta\omega_n = |\mathrm{Im}\ \omega_n|$ is such that $\sigma_n(\mathrm{Re}\ \omega_n \pm \Delta\omega_n) = \sigma_n(\mathrm{Re}\ \omega_n)/2$.

V. 1D-PHOTONIC CRYSTALS

With reference to Fig. 1, let us now consider a symmetric 1D-PBG structure which consists of N periods plus one layer; every period is composed of two layers respectively with lengths h and l and with refractive indices n_h and n_l, while the added layer is with parameters h and n_h. The symmetric 1D-PBG structure consists of $2N+1$ layers with a total length $d = N(h+l)+h$. If the two layers external to the symmetric 1D-PBG structure are considered, the 1D-space x can be divided into $2N+3$ layers; they are $L_k = [x_k, x_{k+1}]$, $k = 0, 1, \ldots, 2N+1, 2N+2$, with $x_0 = -\infty$, $x_1 = 0$, $x_{2N+2} = d$, and $x_{2N+3} = +\infty$. The refractive index $n(x)$ takes a constant value n_k in every layer L_k, $k = 0, 1, \ldots, 2N+1, 2N+2$, i.e.,

$$n(x) = \begin{cases} n_0, & \text{for } x \in L_0,\ L_{2N+2}, \\ n_h, & \text{for } x \in L_k,\ k = 1,3,\ldots,2N-1,2N+1, \\ n_l, & \text{for } x \in L_k,\ k = 2,4,\ldots,2N. \end{cases} \tag{47}$$

As recently described in [6], for symmetric 1D-PBG structures, the expression of the complex norm of a generic QNM functions $\langle f_n | f_n \rangle$ can be obtained in a very simple manner as a derivation process by using an auxiliary function method, instead of an integration [as intuitively suggested by the expression (6)]. Since in these hypothesis the calculation of the norm is rather simple, if we define

$$\gamma_n = \frac{\langle f_n | f_n \rangle}{2i\sqrt{\rho_0}}, \tag{48}$$

the normalized intensity of the nth QNM, i.e., $|f_n^N(x)|^2 = |f_n(x)|^2 |2\omega_n / \langle f_n | f_n \rangle|$, can be reexpressed as $|f_n^N(x)|^2 = (1/\sqrt{\rho_0}) |\omega_n / \gamma_n| |f_n(x)|^2$, and the decay rate (44) and (45), in units of the one in the universe [9], becomes

$$\delta_n(x,\omega) = \frac{1}{2} \left| \frac{\omega_n}{\gamma_n} \right| |f_n(x)|^2 \frac{\sigma_n(\omega)}{K_n \sqrt{\rho_0}},$$

$$\sigma_n(\omega) = \frac{K_n}{\pi d} \frac{|\mathrm{Im}\ \omega_n|}{(\omega - \mathrm{Re}\ \omega_n)^2 + \mathrm{Im}^2\ \omega_n}. \quad (49)$$

As proved in [6], for a quarter wave symmetric 1D-PBG with N periods and ω_{ref} as reference frequency, there are $2N+1$ families of QNMs, i.e., F_n^{QNM}, $n \in [0,2N]$; the F_n^{QNM} family of QNMs consists of infinite QNM frequencies, i.e., $\omega_{n,m}$, $m \in \boldsymbol{Z} = \{0, \pm 1, \pm 2, \ldots\}$, which have the same imaginary part, i.e., $\mathrm{Im}\ \omega_{n,m} = \mathrm{Im}\ \omega_{n,0}$, $m \in \boldsymbol{Z}$, and are lined with a step $\Delta = 2\omega_{ref}$, i.e., $\mathrm{Re}(\omega_{n,m}) = \mathrm{Re}(\omega_{n,0}) + m\Delta$, $m \in \boldsymbol{Z}$. It follows that, if the complex plane is divided into some ranges, i.e., $S_m = \{m\Delta < \mathrm{Re}\ \omega < (m+1)\Delta\}$, $m \in \boldsymbol{Z}$, each of the QNM family F_n^{QNM} drops only one QNM frequency over the range S_m, i.e., $\omega_{n,m} = (\mathrm{Re}\ \omega_{n,0} + m\Delta, \mathrm{Im}\ \omega_{n,0})$; there are $2N+1$ QNM frequencies over the range S_m and they can be referred as $\omega_{n,m} = \omega_{n,0} + m\Delta$, $n \in [0,2N]$. The QNM frequencies are not uniformly distributed in the complex plane, but they arrange themselves in order to form permitted and forbidden bands, in agreement with the known characteristics of these structures [8]. Moreover, the more the 1D-PBG presents a large number of periods ($L > \lambda_{ref}$) with an high refractive index step ($n_h - n_l > n_0$), the more the nth QNM frequency $\omega_{n,0}$ describes the nth transmission peak in the sense that $\mathrm{Re}(\omega_{n,0})$ comes near to the resonance frequency of the nth transmission peak, $|\mathrm{Im}(\omega_{n,0})|$ approximates the FWHM of the nth transmission peak, and $|f_n(x)|^2$ approximates the field intensity distribution inside the 1D-PBG structure at the nth transmission peak [6].

The norm (48) of the QNM $|n,m\rangle$ with frequency $\omega_{n,m} = \omega_{n,0} + m\Delta$ becomes $\gamma_{n,m} = \langle f_{n,m} | f_{n,m} \rangle / 2i\sqrt{\rho_0}$, such that

$$\gamma_{n,m} = \frac{\gamma_{n,0}}{\omega_{n,0}} \omega_{n,m} = \frac{\gamma_{n,0}}{\omega_{n,0}} (\omega_{n,0} + m\Delta). \quad (50)$$

The nth QNM family is such that the $\gamma_{n,m}$ norm is periodic with a step $\Gamma_n = \gamma_{n,0}(\Delta / \omega_{n,0})$. In Ref. [6] all the simplified expressions of relations (48) and (50) in terms of two particular coefficients of an auxiliary functions can be found.

So, for the symmetric 1D-PBG (47) with quarter wave stacks $n_h h = n_l l = \lambda_{ref}/4$, the decay rate (49) of a dipole in the point x, coupled to the QNM $|n,m\rangle$ becomes

$$\delta_{n,m}(x,\omega) = \frac{1}{2} \left| \frac{\omega_{n,0}}{\gamma_{n,0}} \right| |f_{n,m}(x)|^2 \frac{\sigma_{n,m}(\omega)}{K_{n,m}\sqrt{\rho_0}},$$

$$\sigma_{n,m}(\omega) = \frac{K_{n,m}}{\pi d} \frac{|\mathrm{Im}\ \omega_{n,0}|}{(\omega - \mathrm{Re}\ \omega_{n,0} - m\Delta)^2 + \mathrm{Im}^2\ \omega_{n,0}}. \quad (51)$$

Since in the 1D-PBG of length d, the dipole is coupled with the QNM $|n,m\rangle$, at a frequency resonance $\mathrm{Re}\ \omega_{n,m} = \mathrm{Re}\ \omega_{n,0} + m\Delta \geqslant 0$, if we consider the narrow band $\Delta\omega_n = 2|\mathrm{Im}\ \omega_{n,0}| \ll \mathrm{Re}\ \omega_{n,m}$, we can evaluate the normalization constant $K_{n,m}^{(\sigma)}$ in Eq. (51) by using the following condition:

$$\int_{\mathrm{Re}\ \omega_{n,0} + m\Delta - |\mathrm{Im}\ \omega_{n,0}|}^{\mathrm{Re}\ \omega_{n,0} + m\Delta + |\mathrm{Im}\ \omega_{n,0}|} \sigma_{n,m}(\omega) d\omega = \frac{1}{d}. \quad (52)$$

As an example let us consider a symmetric quarter wave 1D-PBG, with reference wavelength $\lambda_{ref} = 1\ \mu$m, number of periods $N = 5$, refractive indices $n_h = 2$ and $n_l = 1.5$. There are $2N+1$ QNMs in the $[0, 2\omega_{ref}]$ range. In the hypothesis of single resonance, a dipole inside the structure can be coupled to just one of these QNMs, which are $|n\rangle = |n,0\rangle$ with $n \in [0,2N]$.

In Figs. 2, the QNM intensities $I_n = |f_{n,0}(x)|^2$ [6], in units of the maximum value $I_{\max}$ inside the 1D-PBG, are plotted as a function of the dimensionless space x/d, where d is the length of the structure, for (a) the QNM $|3\rangle$, having the frequency closed to the first transmission peak before the first band edge, (b) the QNM $|4\rangle$, corresponding to the low-frequency band edge, (c) the QNM $|5\rangle$, corresponding to the high-frequency band edge, and (d) the QNM $|6\rangle$, closed to the first transmission peak after the high-frequency band edge. When we speak about frequency, we usually refer to the real part of the frequency ω_n, if not otherwise specified. The QNMs corresponding to the two band edges present the largest intensities in the 1D-PBG. The QNM intensity I_n has $n+1$ minima. In the center of the structure $x = d/2$, the QNM intensities have a maximum for odd values of n and are null for even values of n and, on the two surfaces of the cavity, $x = 0$ and $x = d$, all the graphs show the same value for the (relative) intensity. Finally, I_N is almost null in the range in which there is a maximum of I_{N-1}, and I_{N-1} is small in the range in which there is the second relative maximum of I_N.

In Fig. 3, the DOM according to the QNM theory [6] is plotted as a function of the dimensionless frequency ω/ω_{ref} and is normalized to a bulk velocity v_{bulk}, which corresponds to scaling the DOM by that of an infinite homogeneous material with an effective index that is the harmonic mean of n_h and n_l [20]. The photonic band gap is in a region $\omega/\omega_{ref} = [0.84, 1.16]$; the suppression of the DOM in the gap is clear, as the enhancement of the DOM at the band-edge resonances $\omega_{low}/\omega_{ref} = 0.84$ and $\omega_{high}/\omega_{ref} = 1.16$, where the spectral transmission is one; there are other less-pronounced peaks in the DOM on the pass-band at the frequencies that correspond to other transmission resonances [20].

In Figs. 4, decay rates $R_n = \delta_{n,0}(x,\omega)$, (51) in units of the maximum value $R_{\max}$ inside the 1D-PBG, are plotted as a function of the dimensionless space x/d and the dimensionless frequency ω/ω_{ref} for (a) R_3, the coupling dipole-QNM $|3\rangle$ having the frequency closed to the first transmission peak before the low frequency band edge, (b) $|4\rangle$, i.e., the coupling dipole-QNM corresponding to the low-frequency band edge, (c) R_5, the coupling dipole-QNM $|5\rangle$ corresponding to the high-frequency band edge, and (d) R_6, the coupling dipole-QNM $|6\rangle$ corresponding to the next transmission peak after the high frequency band edge. The decay rates R_4 and R_5, corresponding to the two band edges, stand out respect to R_3 and R_6 of the next transmission peaks, because, in the two band-edge resonances, the DOM is enhanced (Fig. 3) and the QNMs present the most large intensities inside the structure (Fig. 2). Moreover, the decay rate R_n is centered around the QNM frequency ω_n and, like the QNM intensity I_N, has $n+1$ minima along the x direction (Fig. 2). We note that the QNM approach uses a realistic model for the 1D-PBG, as a finite cavity with discontinuities in the refractive index, so

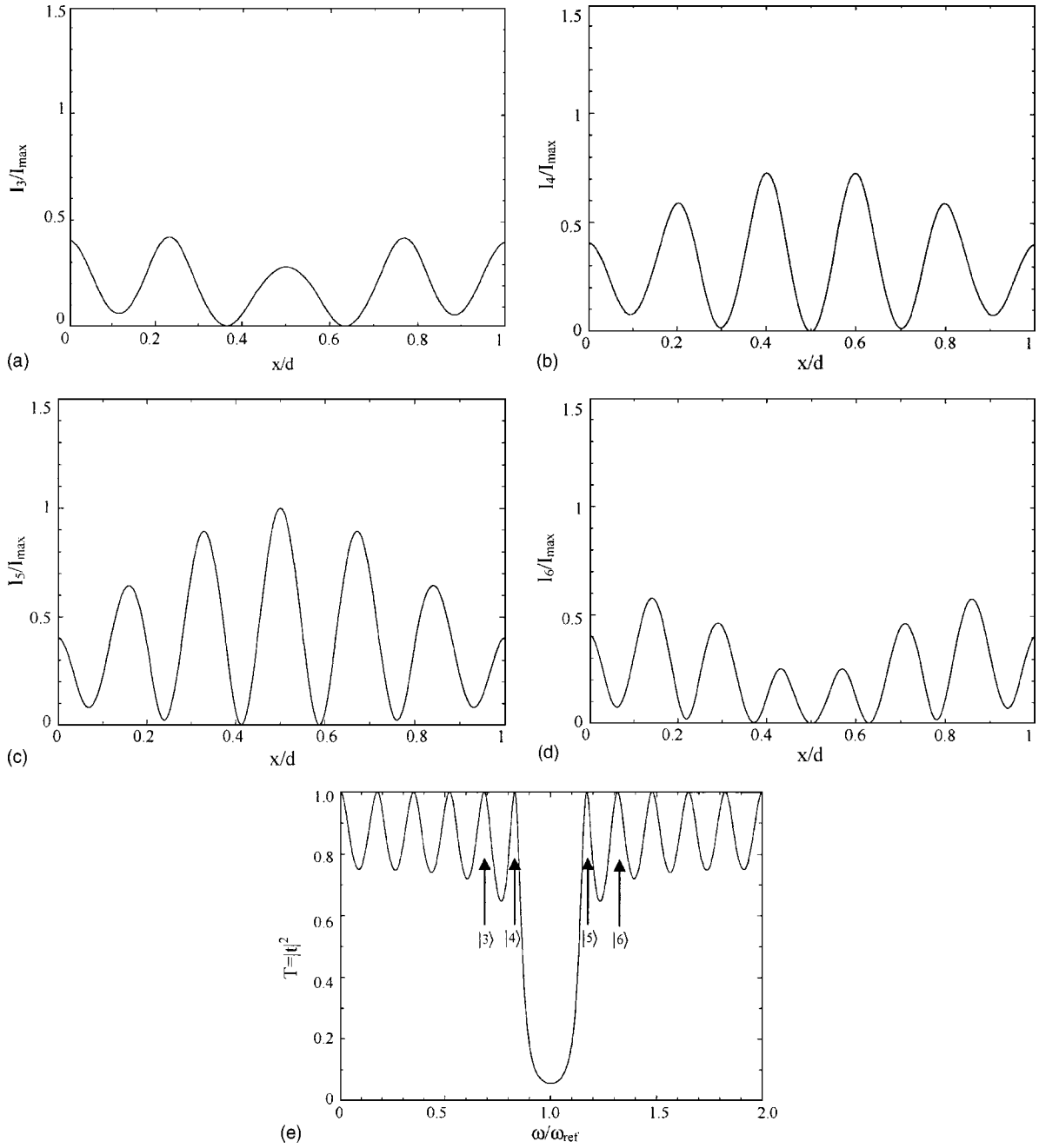

FIG. 2. QNM wave function intensities $I_n=|f_{n,0}(x)|^2$ [5], in units of the maximum intensity $I_{\max}$, inside the 1D-PBG structure, plotted as a function of the dimensionless space x/d, where d is the length of the cavity. The 1D-PBG structure is symmetric, with quarter wave stacks: reference wavelength $\lambda_{ref}=1$ μm, number of periods $N=5$, refractive indices $n_h=2$ and $n_l=1.5$. In the $[0,2\omega_{ref}]$ range there are $2N+1$ QNMs, as well as the transmission peaks [6], i.e., $|n\rangle=|n,0\rangle$ with $n\in[0,2N]$. (a) Intensity for QNM $|3\rangle$, having the real part of the frequency centered in $\omega/\omega_{ref}=0.6891$ [see Fig. 2(e)]; (b) intensity for QNM $|4\rangle$, corresponding to the low-frequency band edge $\omega/\omega_{ref}\cong 0.8397$ [see Fig. 2(e)]; (c) intensity for QNM $|5\rangle$, corresponding to the high-frequency band edge $\omega/\omega_{ref}\cong 1.160$ [see Fig. 2(e)]; (d) intensity for QNM $|6\rangle$, having the real part of the frequency centered in $\omega/\omega_{ref}=1.311$ [see Fig. 2(e)]; (e) transmission spectrum for a symmetric quarter-wave 1D-PBG, with reference wavelength $\lambda_{ref}=1$ μm and number of periods $N=5$, refractive indices $n_h=2$ and $n_l=1.5$.

this approach improves the results of the paper [19], obtained by the Kronig-Penney model.

In Figs. 5, the decay rates R_n, in units of the maximum value $R_{\max}$ inside the 1D-PBG, are plotted as functions of the dimensionless frequency ω/ω_{ref} when (a) the dipole is in the center of the structure $x=d/2$ or (b) on the surfaces $x=0$ and $x=d$. Moreover, the decay rates R_4 and R_5, corresponding to the band edges, and R_3, R_6, of the two next transmission peaks, are plotted when the dipole is inside the 4th period of the cavity and is put (c) on the center of the high index layer $x=(d/2)+(\delta/2)$ or (d) on the center of the low index layer $x=(d/2)+\delta$, where $\delta=h+l$. In all Figs. 5(a)–5(d), the decay rate is strongly suppressed in the band gap $\omega/\omega_{ref}=[0.84,1.16]$, since the DOM is suppressed here (Fig. 3).

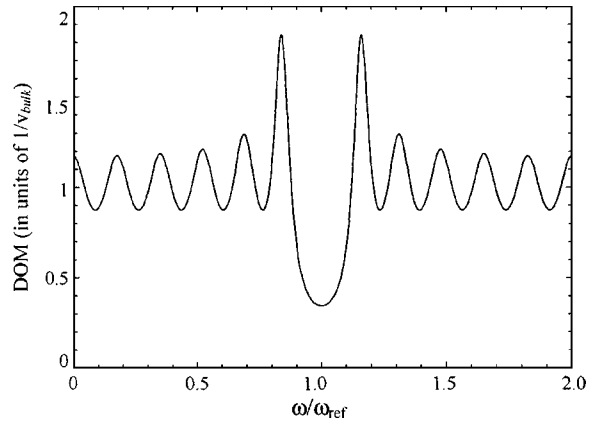

FIG. 3. Density of modes (DOM) according to the QNM theory, for a symmetric 1D-PBG with quarter wave stacks: reference wavelength $\lambda_{ref}=1$ μm, number of periods $N=5$, refractive indices $n_h=2$ and $n_l=1.5$ [5]. The DOM is plotted as a function of the dimensionless frequency ω/ω_{ref} and is normalized to a bulk velocity v_{bulk}, which corresponds to scaling the DOM by that of an infinite homogeneous material with an effective index that is the harmonic mean of n_h and n_l [20].

When the dipole is in the center $x=d/2$ of the 1D-PBG [Fig. 5(a)]: the dipole can be coupled just to the QNMs $|n\rangle$ with an odd n, because, in $x=d/2$, the QNM intensities I_n have a maximum for odd values of n and are null for even value of n (Fig. 2); moreover, the decay rate R_5, corresponding to the high band edge, presents the maximum peak $R_{\max}$, as it could be intuitively suggested by the placement of the dipole inside the symmetric 1D-PBG. For the 1D-PBG with the parameters above considered, $\lambda_{ref}=1$ μm, $N=5$, $n_h=2$ and $n_l=1.5$, the ratio between $R_{\max}$ and the peak of the emission rate R_7 is 2.152.

When the dipole is on the surfaces $x=0$ and $x=d$ of the structure [Fig. 5(b)]: the dipole can be coupled to all the QNMs $|n\rangle$, in fact the QNM intensities I_n are not null on $x=0$ and $x=d$ (Fig. 2); moreover, the peaks of the decay rates R_4 and R_5, corresponding to the two band edges, present similar values on the peaks of the decay rates R_n, corresponding to the other transmission resonances, as it could be intuitively suggested [all the QNM intensities I_n have the same values in $x=0$ and $x=d$ (Fig. 2)]. For the 1D-PBG with the parameters above considered, the peak of the decay rates $R_{4,5}$, in unit of $R_{\max}$, is 0.4052; instead, the ratio between the $R_{4,5}$ peak and the $R_{3,6}$ peak is 0.9491.

When the dipole is inside the 4th period of the cavity, if it is put on the center of the high index layer $x=(d/2)+(\delta/2)$ [Fig. 5(c)]: the decay rate R_4, corresponding to the low-frequency band edge, is enhanced, because, in $x=(d/2)+(\delta/2)$, the intensity I_4 of the QNM $|4\rangle$ is maximum (Fig. 2); moreover, the decay rate R_5, corresponding to the high-

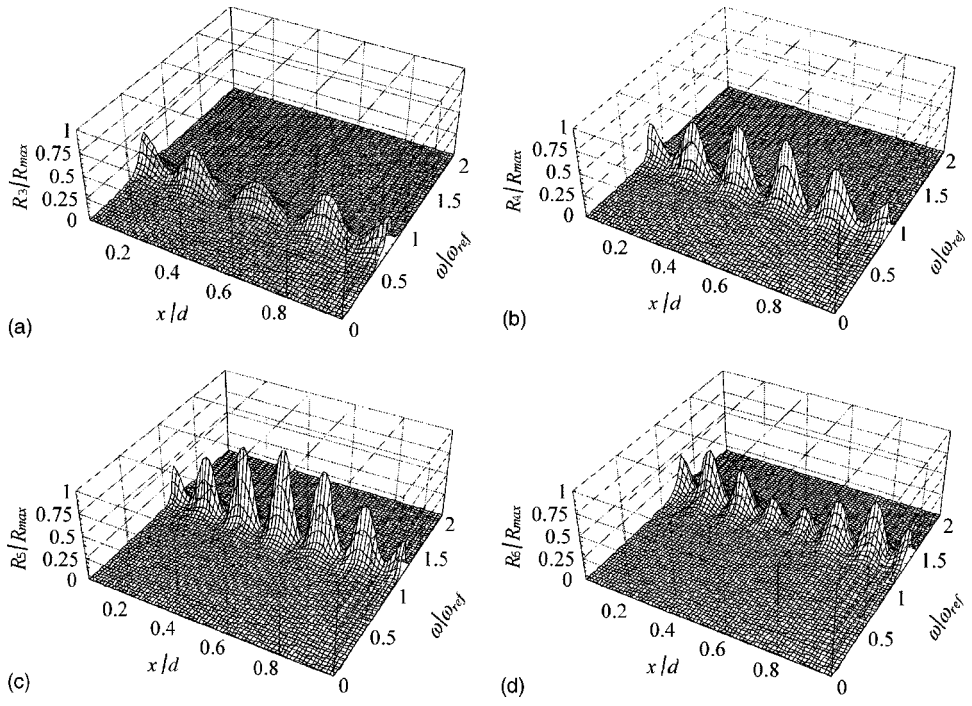

FIG. 4. Decay rates $R_n=\delta_{n,0}(x,\omega)$ (51), in units of the maximum decay rate $R_{\max}$, inside the 1D-PBG structure, plotted as a function of the dimensionless space x/d, where d is the length of the cavity, and as function of the dimensionless frequency ω/ω_{ref}, where ω_{ref} is the reference frequency of the cavity. The 1D-PBG structure is symmetric, with quarter wave stacks: reference wavelength $\lambda_{ref}=1$ μm, number of periods $N=5$, refractive indices $n_h=2$ and $n_l=1.5$. In the conservative limit [12], the dipole can be coupled to just one of the $2N+1$ QNMs in the $[0,2\omega_{ref}]$ range, which we can indicate with $|n\rangle=|n,0\rangle$ and $n\in[0,2N]$. In (a) is reported decay rate R_3, for the coupling dipole-QNM $|3\rangle$ [corresponding to the frequency depicted in Fig 2(a)]; in (b) is printed the decay rate R_4, for the coupling dipole-QNM $|4\rangle$ [corresponding to the low-frequency band edge; see Fig. 2(b)]; in (c) is reported the decay rate R_5 for the coupling dipole-QNM $|5\rangle$ [corresponding to the high-frequency band edge; see Fig. 2(c)] and in (d) is printed the decay rate R_6, for the coupling dipole-QNM $|6\rangle$ [having the real part of the frequency corresponding to the transmission peak reported in Fig. 2(d)].

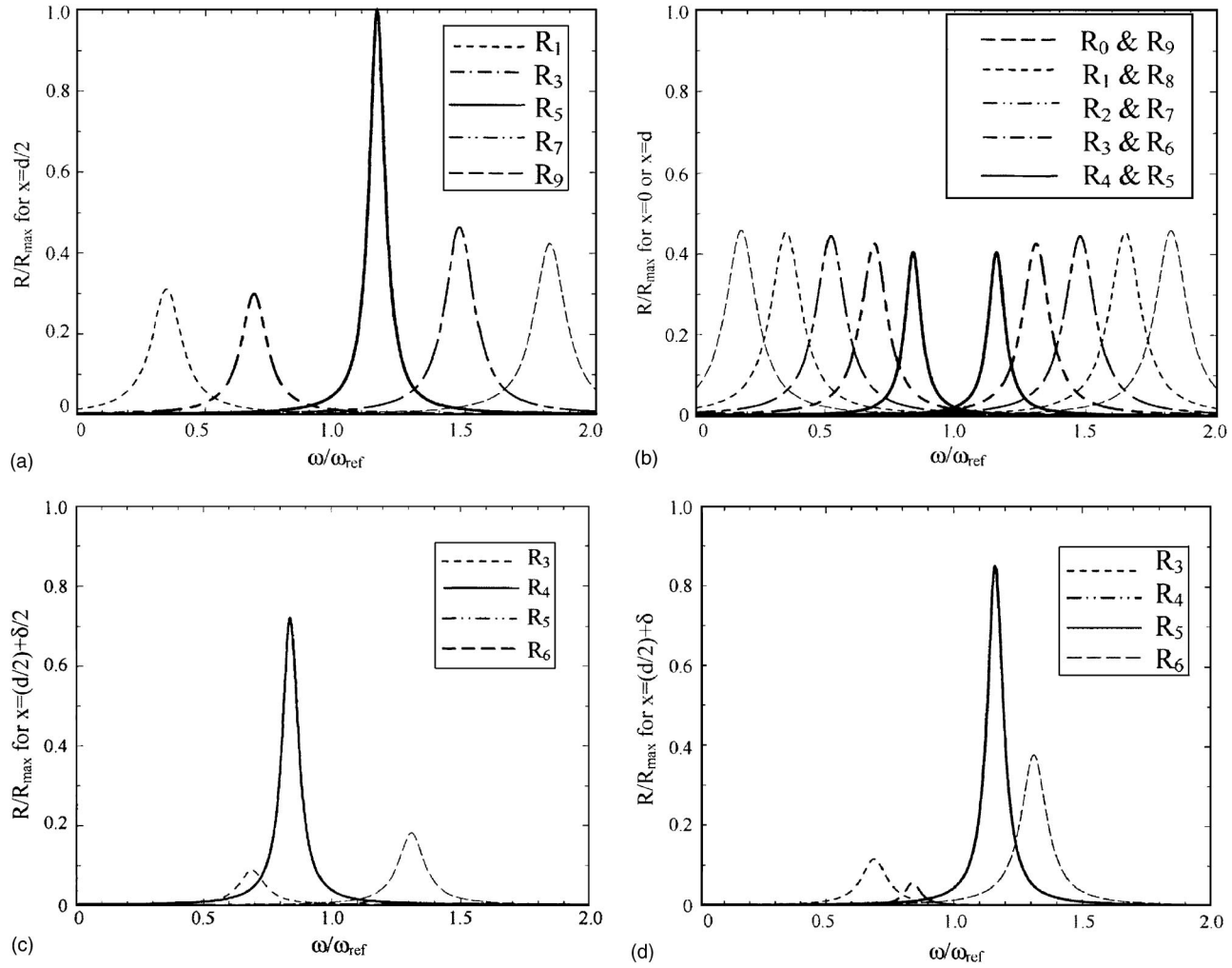

FIG. 5. For a symmetric quarter wave 1D-PBG, with $\lambda_{ref}=1$ μm, $N=5$, $n_h=2$, and $n_l=1.5$, a dipole is coupled just to one of the $2N+1$ QNMs in the $[0,2\omega_{ref}]$ range, which we have indicated by $|n\rangle$ with $n\in[0,2N]$. The decay rates R_n with $n\in[0,2N]$, in units of the maximum value $R_{\max}$ inside the 1D-PBG, are plotted as functions of the dimensionless frequency ω/ω_{ref} when (a) the dipole is in the center of the cavity $x=d/2$; (b) the dipole is on one of the two surfaces $x=0$ and $x=d$. In (c) and (d) the decay rates R_4 and R_5, corresponding to the band edges [see Figs. 2(b) and 2(c)], and R_3, R_6, corresponding to the two next transmission peaks [see Figs. 2(a)–2(d)], are plotted when the dipole is inside the 4th period of the 1D-PBG and it is exactly (c) in the center of the high index layer $x=(d/2)+(\delta/2)$; (d) in the center of the low index layer $x=(d/2)+\delta$, where $\delta=h+l$.

frequency band edge, is almost suppressed, because, even if the DOM is large (Fig. 3), the QNM intensity I_5 is almost null in the maximum of the QNM intensity I_4 (Fig. 2). For the 1D-PBG with the parameters above considered, the peak of the decay rate R_4, in unit of $R_{\max}$, is 0.7208; instead, the peak ratio R_4/R_5 is 64.11 and the peak ratio R_4/R_3 is much smaller, i.e., 8.162.

If the dipole is put on the center of the low index layer $x=(d/2)+\delta$ [Fig. 5(d)]: the decay rate R_5, corresponding to the high-frequency band edge is enhanced, because, in $x=(d/2)+\delta$, the intensity I_5 of the QNM $|5\rangle$ have a relative maximum (Fig. 2); moreover, the decay rate R_4, corresponding to the low-frequency band edge, is decreased, because, even if the DOM is large (Fig. 3), the QNM intensity I_4 is small in the second relative maximum of the QNM intensity I_5 (Fig. 2). For the 1D-PBG with the parameters above considered, the peak of the decay rate R_5, in unit of $R_{\max}$, is 0.8519; instead, the peak ratio R_5/R_4 is 14.78 and the peak-ratio R_5/R_6 is not too smaller, i.e., 2.245. The QNM approach to calculate the decay rate for a dipole in a 1D-PBG structure presents the advantage to develop a general quantum treatment. This approach agrees with the theoretical results of the paper [19], that considers only a classical model. Moreover, the approach confirms the results of the paper [21], that is only a numerical investigation.

VI. CONCLUSIONS

In this work we take into consideration one-dimensional finite PBG structures (1D-PBG), i.e., finite length optical cavities, with both sides open to an external environment and containing a layered material inside. In the general case these structures cannot be studied as infinite structures, but we have to consider the boundary conditions at the two ends. Electromagnetic field in these structures is well described by using an extension of the quasinormal modes (QNM) theory

[6], first applied to optical cavities by Leung *et al.* [1–8]. This theory provides a very good approach to this problem from a classical standpoint, in fact the lack of energy conservation for the cavity gives rise to complex (instead of real) eigenfrequencies for the field. Since the space-time evolution operator for the field inside the cavity is not Hermitian, fields modes cannot be considered normal (i.e., coming from stationary conditions) but they are called quasinormal and the QNM theory well covers this topic. QNM approach is very different from the pseudomodes one introduced by Dalton *et al.* [11]. In fact, the pseudomodes are obtained by the Fano transformation of the normal modes [12], so they use an ordinary metric and the canonical second quantization is adopted; QNM do not, they use a specific definition for the norm (metric) and so a noncanonical second quantization is adopted (see Refs. [5,8,9]). In the paper [9], the quantization of the optical cavity on a quasinormal modes base was been done considering a mirror in one of the two sides of the cavity; in this paper we have generalized the second quantization scheme for double open optical cavities (removing the nodal field condition at one end of the structure) specifying the treatment for PBG structures in which field can enter and to go out from both sides. Various physical quantities are then written as diagonal or nondiagonal sums over QNM base. We wrote down the operatorial expansion of the field, inside the cavity, in terms of quasinormal functions and operators, extending the second quantization QNM-based scheme [7]. We have introduced the Feynman's propagator, in terms of QNM, in order to describe the decay rate of a dipole inside this finite structure. The resonance approximation is studied, verifying the enhancement of the decay rate of excited states related to the behaviors of the equal-space propagator $\tilde{D}(x,\omega)$. In several numerical simulations we point out the links between the decay rate of the atom and the quasi normal modes involved inside the cavity. The quantum QNM approach to the calculation of the decay rate of a dipole in 1D-PBG agrees with the theoretical results of the paper [19], that considers only classical models. Moreover, this approach confirms the results of the paper [21], that is only a numerical investigation. Non-Hermitian Hamiltonians and ensuing complex eigenvalues also figure prominently in Siegman's work on dissipative CQED [28], but these works are semiclassical treatments in which the fields are considered as *c* number, and the limit $\lambda \ll d$ is considered, where λ is the wavelength and d is the dimension of the structure. The present paper goes beyond these limits, working in a different regime; the main results of this paper consist, at first, in the introduction of the second quantization scheme for photonic crystals viewed as open systems, by using the QNM theory. Then, using the just mentioned formalism, we study the decay rate of an atom situated inside the crystal performed by the Feynman propagator expressed in terms of quasinormal functions. The formalism used in Secs. II and III, in particular the introduction of the two driving forces $b_{left}(t)$ and $b_{right}(t)$, is an useful and well defined method for any initial state of the fields. Taking a coherent state instead of a thermal one, enables the study of a (general counter-propagating) pumped cavity.

The general version of this theory, as presented in the first three sections, could be applied to a large variety of optical systems studied in the framework of the double-sides open systems, i.e., for future developments about photonic crystals (and more general optical devices) this paper could serve as a reference on the subject.

ACKNOWLEDGMENT

The authors would like to thank Professor B. J. Hoenders for the interesting discussions about the quasinormal modes theory.

[1] K. Sakoda, *Optical Properties of Photonic Crystals* (Springer-Verlag, Berlin, 2001); J. Maddox, Nature (London) **348**, 481 (1990); S. John, Phys. Rev. Lett. **58**, 2486 (1987); **53**, 2169 (1984).

[2] P. Yeh, *Optical Waves in Layered Media* (Wiley, New York, 1988).

[3] M. Centini, C. Sibilia, M. Scalora, G. D'Aguanno, M. Bertolotti, M. J. Bloemer, C. M. Bowden, and I. Nefedov, Phys. Rev. E **60**, 4891 (1999).

[4] J. E. Sipe, L. Poladian, and C. Martijn de Sterke, J. Opt. Soc. Am. A **4**, 1307 (1994).

[5] P. T. Leung, S. Y. Liu, and K. Young, Phys. Rev. A **49**, 3057 (1994); P. T. Leung, S. S. Tong, and K. Young, J. Phys. A **30**, 2139 (1997); **30**, 2153 (1997).

[6] A. Settimi, S. Severini, N. Mattiucci, C. Sibilia, M. Centini, G. D'Aguanno, M. Bertolotti, M. Scalora, M. Bloemer, and C. M. Bowden, Phys. Rev. E **68**, 026614 (2003).

[7] K. C. Ho, P. T. Leung, Alec Maassen van den Brink, and K. Young, Phys. Rev. E **58**, 2965 (1998).

[8] E. S. C. Ching, P. T. Leung, A. Maassen van der Brink, W. M. Suen, S. S. Tong, and K. Young, Rev. Mod. Phys. **70**, 1545 (1998).

[9] S. Weinberg, *The Quantum Theory of Fields* (Cambridge University Press, New York, 1996); A. A. Abrikosov, L. P. Gor'kov, and I. E. Dzyaloshinski, *Methods of Quantum Field Theory in Statistical Physics* (Dover, New York, 1975); C. Choen-Tannoudji, J. Dupont-Roc, and G. Grynberg, *Photons and Atoms—Introduction to Quantum Electrodynamics* (Wiley, New York, 1997).

[10] R. P. Feynman and F. L. Vernon, Ann. Phys. (N.Y.) **24**, 118 (1963); H. Dekker, Phys. Rep. **80**, 1 (1981); P. S. Riseborough, P. Hänggi, and U. Weiss, Phys. Rev. A **31**, 471 (1985).

[11] B. J. Dalton, Stephen M. Barnett, and B. M. Garraway, Phys. Rev. A **64**, 053813 (2001).

[12] H. M. Lai, P. T. Leung, and K. Young, Phys. Rev. A **37**, 1597 (1988).

[13] I. Takahashi and K. Ujihara, Phys. Rev. A **56**, 2299 (1997).

[14] Z. Huang, C. Lei, D. G. Deppe, C. C. Lin, C. J. Pinzone, and R. D. Dupuis, Appl. Phys. Lett. **61**, 2961 (1992).

[15] Xiao-Ping Feng and Kikuo Ujihara, Phys. Rev. A **41**, 2668 (1990).
[16] E. Yablonovitch, Phys. Rev. Lett. **58**, 2059 (1987); E. Yablonovitch and T. J. Gmitter, *ibid.* **63**, 1950 (1989).
[17] E. M. Purcell, Phys. Rev. **69**, 681 (1946).
[18] G. Kurizki and A. Z. Genack, Phys. Rev. Lett. **61**, 2269 (1988); G. Kurizki, Phys. Rev. A **42**, 2915 (1990).
[19] J. P. Dowling, J. Lightwave Technol. **17**, 2142 (1999); J. P. Dowling and C. M. Bowden, Phys. Rev. A **46**, 612 (1992).
[20] J. M. Bendickson, J. P. Dowling, and M. Scalora, Phys. Rev. E **53**, 4107 (1996); I. S. Fogel, J. M. Bendickson, M. D. Tocci, M. J. Bloemer, M. Scalora, C. M. Bowden, and J. P. Dowling, Pure Appl. Opt. **7**, 393 (1998).
[21] M. Scalora, J. P. Dowling, M. Tocci, M. J. Bloemer, C. M. Bowden, and J. W. Haus, Appl. Phys. B: Lasers Opt. **60**, S57 (1995).
[22] R. Banerjee and P. Mukherjee, J. Phys. A **35**, 5591 (2002).
[23] G. Wentzel, *Quantum Theory of Fields* (Interscience, New York, 1949).
[24] H. Arthur Weldon, Phys. Rev. D **53**, 7265 (1996).
[25] R. Feynman, *Quantum Electrodynamics* (Benjamin, New York, 1962).
[26] M. Ueda and I. Nobuyuki, Phys. Rev. A **50**, 89 (1994).
[27] A. Lahiri and P. B. Pal, *A First Book of Quantum Field Theory* (CRC Press, Calcutta, 2000).
[28] A. E. Siegman, Phys. Rev. A **39**, 1253 (1989); **39**, 1264 (1989); A. G. Fox and T. Li, Bell Syst. Tech. J. **40**, 453 (1961).